Geomorphic constraints on surface uplift, exhumation, and plateau growth in the Red River region, Yunnan Province, China

L.M. Schoenbohm[†]
K.X Whipple
B.C. Burchfiel
Massachusetts Institute of Technology, Department of Earth, Atmospheric and Planetary Sciences, 77 Massachusetts Ave., Cambridge, Massachusetts 02139, USA

L. Chen
Yunnan Institute of Geological Sciences, 131 Baita Rd., Kunming, Yunnan, China

ABSTRACT

Field observations, digital elevation model (DEM) data, and longitudinal profile analysis reveal a perched low-relief upland landscape in the Red River region, Yunnan Province, China, which correlates to an uplifted, regional low-relief landscape preserved over the eastern margin of the Tibetan Plateau. As with other major rivers of the plateau margin, the Red River has deeply incised the low-relief upland landscape, which we interpret to be the remnants of a pre-uplift or relict landscape. We examine longitudinal river profiles for 97 tributaries of the Red River. Most profiles consist of three segments separated by sharp knickpoints: an upper, low-gradient channel segment, a steeper middle channel segment, and a very steep lower channel segment. Upper channel segments correspond to the relict landscape and have not yet experienced river incision. Steeper middle and lower segments indicate onset of rapid, two-phase river incision, on the basis of which changes in external forcings, such as climate or uplift, can be inferred. In terms of two end-member scenarios, two-phase incision could be the result of pulsed plateau growth, in which relatively slow uplift during the first phase is followed by rapid uplift during the second phase, or it could reflect adjustments of the main channel to changing climate conditions against the backdrop of steady plateau growth. Reconstruction of the paleo–Red River indicates ~1400 m river incision, 1400–1500 m surface uplift, and a maximum of 750 m vertical displacement across the northern Red River fault, elevating the northern Ailao Shan range above the surrounding relict landscape. On the basis of stratigraphic constraints, incision along the Red River likely began in Pliocene time.

Keywords: Asia, landscape evolution, Red River fault, Ailao Shan shear zone, erosion surface, fluvial geomorphology, incision.

INTRODUCTION

Tectono-geomorphic studies have yielded valuable insights in Asia, where continental scale strike-slip faults, extensive crustal thickening, surface uplift, and regional climatic interactions have shaped the dramatic modern landscape (Hallet and Molnar, 2001; Clark, 2003; Clark et al., 2004). The eastern margin of the Tibetan Plateau has experienced extensive deformation associated with the India-Asia collision, particularly along the Ailao Shan shear zone and the Red River fault in southeast China and Vietnam (Fig. 1). A number of studies have focused on the Ailao Shan shear zone (Harrison et al., 1992; Leloup and Kienast, 1993; Schärer et al., 1994; Leloup et al., 1995, 2001; Harrison et al., 1996; Wang, P.L., et al., 1998, 2000; Zhang and Schärer, 1999), and some work has evaluated the Red River fault (Allen et al., 1984; Wang, E., et al., 1998; Replumaz et al., 2001). Absent in this research, however, is a significant consideration of the regional geomorphology.

In this study, we combine field observations with topographic data to understand aspects of the Cenozoic structural and geomorphic evolution of the Red River region of Yunnan Province, China. Geomorphic observations of the landscape can enhance our understanding of the regional geology and constrain tectonic models, specifically, interactions among the active fault systems, the regional uplift history, and aspects of the unroofing history of the shear zone. We describe locally a low-relief upland landscape, continuous with a regional low-relief upland landscape developed over the eastern plateau margin (Clark, 2003), which is deeply incised by the Red River. We reconstruct the paleo–Red River tributary network developed on the low-relief landscape, and use these data to constrain the amount of surface uplift experienced in the Red River region, and the amount and distribution of dip-slip displacement on the Red River fault. Tributary morphology and channel parameters also allow us to explore geodynamic and climatic aspects of the landscape evolution of this region.

GEOLOGIC SETTING

The study area, in Yunnan Province, China, lies east of the Eastern Himalayan Syntaxis and is currently affected by right-lateral shear and clockwise rotation as India moves northward into the Eurasian continent (Cobbold and Davy, 1988; Davy and Cobbold, 1988; Dewey et al., 1989; Holt et al., 1991; Wang and Burchfiel, 1997; Wang, E., et al., 1998; Hallet and Molnar, 2001). The Red River fault and Ailao Shan shear zone are products of this deformation.

The Oligo-Miocene Ailao Shan shear zone consists of four segments in China and Vietnam (Fig. 1). The vertically foliated gneisses of the Ailao Shan segment are bounded on the northeast by the active Red River fault and on the southwest by the probably inactive Ailao Shan fault (Fig. 1). Shearing began ca. 34 Ma (Gilley et al., 2003) and was followed by rapid cooling

[†]Present address: Universität Potsdam, Institut für Geowissenschaften, Postfach 60 15 53, Haus 25, Potsdam D-14415, Germany; e-mail: lindsays@geo.uni-potsdam.de.

GSA Bulletin; July/August 2004; v. 116; no. 7/8; p. 895–909; doi: 10.1130/B25364.1; 7 figures; 2 tables; Data Repository item 2004104.

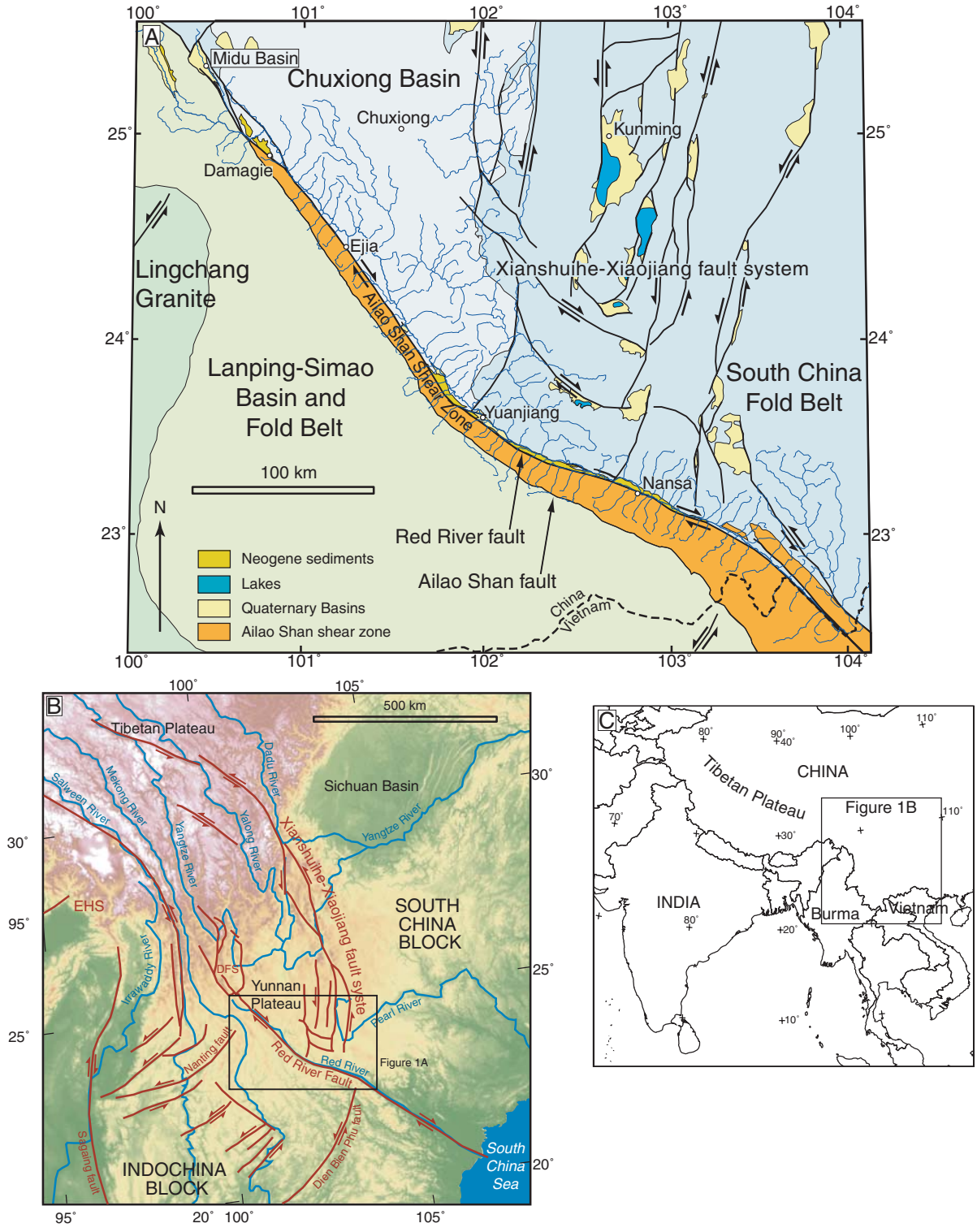

Figure 1. (A) Geologic map of field area. South China block shown in shades of blue, Indochina block in shades of green, separated by the Ailao Shan shear zone and Red River fault. The South China fold belt is of mixed lithology, but in the vicinity of the Red River contains massive Triassic limestones. Chuxiong basin rocks are dominantly Mesozoic to early Cretaceous sedimentary rocks, as are rocks of the Lanping-Simao fold-and-thrust belt. The Red River drainage network is traced in blue. Active faults are marked with a heavy-weight black line. The inactive Ailao Shan fault, which marks the southern boundary of the Ailao Shan shear zone, is shown with a medium-weight line. (B) Map of the eastern margin of the Tibetan Plateau. EHS—Eastern Himalayan Syntaxis, DFS—Dali fault system. Data for map from ~1 km resolution GTOPO30 DEM (U.S. Geological Survey, 1993). The Yunnan Plateau is a physiographic feature, part of the southeastern margin of the Tibetan Plateau. Figure 1A location indicated by box. (C) Regional political map showing location of Figure 1B.

between ca. 25 and ca. 17 Ma, diachronous along strike (Harrison et al., 1996). Additional zircon and apatite fission-track data indicate rapid cooling from 13 to 10 Ma (Bergman et al., 1997; Leloup et al., 2001), but it is unclear whether this cooling phase is continuous with that indicated by the Harrison et al. (1996) thermochronology, or if it represents a distinct cooling event. Shear sense indicators are consistently left-lateral (Leloup et al., 1995, 2001), and estimates for the amount of offset fall in the range of 700 ± 200 km (Brias et al., 1993; Leloup et al., 1995, 2001; Wang, P.L., et al., 1998). The Ailao Shan shear zone likely accommodated southward extrusion of Indochina, but the exact nature of the associated crustal deformation is unclear (Tapponnier et al., 1982, 1986, 1990; Leloup et al., 1995, 2001; Wang and Burchfiel, 1997).

In contrast to the ductile, left-lateral Ailao Shan shear zone, the Red River fault (Fig. 1) is a geomorphically prominent, right-lateral structure, approximately bounding the northeastern edge of the shear zone. The fault plane is vertical to slightly east dipping. Strike-slip estimates, based on geomorphic and geologic data, range from 5.5 to 54 km (Allen et al., 1984; Wang, E., et al., 1998; Replumaz et al., 2001). The age of inception is also not well known, but estimates fall in the range 2 to 5 Ma (Allen et al., 1984; Wang, E., et al., 1998; Replumaz et al., 2001). The fault is traceable from Vietnam northwest past the northern segment of the Ailao Shan shear zone and into the Midu basin (Fig. 1). A prominent feature of the Red River fault in map view is a major bend near its intersection with the left-lateral Xianshuihe-Xiaojiang fault system. Northwest of this bend, triangular facets, Quaternary sedimentary basins, and high peak elevations within the Ailao Shan range have been interpreted to result from a dip-slip displacement on the Red River fault with the northeast side down (Allen et al., 1984; Replumaz et al., 2001; Leloup et al., 1995; Wang, E., et al., 1998). Replumaz et al. (2001) observed triangular facets southeast of the bend as well, and on this basis infer that dip-slip displacement extends along the entire length of the fault in China. However, as pointed out by Allen et al. (1984), differential erosion along the gneissic foliation of the Ailao Shan shear zone, which is subvertical but often dips slightly valleyward, can create the appearance of triangular facets in the absence of true dip-slip displacement. Wang, E., et al. (1998) argue that normal faulting does not continue south of the bend. Thus, the amount and distribution of dip-slip along the fault is uncertain but is important in interpreting the way in which the Red River fault interacts with other active fault systems in Yunnan, particularly the Xianshuihe-Xiaojiang fault system, and in constraining the amount of exhumation of the Ailao Shan shear zone along the Red River fault.

In addition to deformation along strike-slip shear zones as a response to the India-Eurasia collision, the eastern margin of Tibet is argued to have experienced long-wavelength surface uplift as a result of pressure gradient–driven flow of weak lower crust from beneath Tibet and inflation of adjacent regions (Royden, 1996; Royden et al., 1997; Clark and Royden, 2000). Surface uplift, exhumation of the Ailao Shan shear zone, and displacement along the Red River fault and other active fault systems of Yunnan have all interacted to shape the modern landscape, which preserves an interpretable record of these processes.

TOPOGRAPHIC SETTING

A regionally extensive, perched, low-relief upland landscape extends from Tibet toward the South China Sea along the southeastern margin of the Tibetan Plateau, and is deeply dissected by major rivers that drain the plateau, including the Mekong, Salween, and Yangtze and their principle tributaries (Fig. 1B; Clark et al., 2002; Clark, 2003). This low-relief upland landscape continues into central and southern Yunnan, where it is incised by the Red River (Figs. 1A and 2; Clark et al., 2002; Clark, 2003). In the Red River region, low-relief landscape patches are generally between 2000 and 2500 m, except for in the northwest Ailao Shan range, where average elevations are closer to 3000 m (Fig. 2A). To the southwest of the Red River, the low-relief landscape is best preserved on the northern segment of the Ailao Shan range and can be traced in discontinuous patches toward the southeast along the crest of the range. To the northeast of the Red River, on the Yunnan Plateau, the low-relief landscape is extensive and is discussed by Wang, E., et al. (1998).

The low-relief upland landscape, where developed on the Ailao Shan range, exhibits a "hummocky" topography with rounded hills separated by meandering, low-gradient, gravel- and sand-bedded streams (Figs. 3 and 4A). Relief is generally less than 200 m but can reach a maximum of 500 m. Everywhere within the low-relief landscape, bedrock is deeply weathered, capped by a saprolite layer estimated to be ~200 m thick. The original gneissic foliation of the Ailao Shan shear zone is well preserved throughout the saprolite, indicating little disruption of the weathered material. Because of the many small hills and the high porosity of the underlying material, the low-relief upland landscape is dry, uncultivated, and sparsely populated. Near Ejia (Figs. 1 and 3), the low-relief upland is developed on Ailao Shan gneiss and lower-grade metamorphic rocks to the west, separated by the Ailao Shan fault (Bureau of Geology, Yunnan, 1990). To the east of the fault, the soil is well-drained saprolite and supports the typical vegetation of the Ailao Shan range, a mixture of grasses and conifers. In contrast, the phyllite to the west of the fault supports a temperate rain forest because the clay-rich soils that have developed on the phyllite better retain moisture (Fig. 3). While the Ailao Shan fault does not appear to be active in a strike-slip sense here or elsewhere along the shear zone, it does form a scarp in this region, higher to the west, probably the result of differential weathering and erosion.

To the northeast of the Red River, the low-relief upland landscape is gently rolling and is developed on a variety of rocks of the Chuxiong basin and South China fold belt (Wang, E., et al., 1998; Figs. 1 and 4B). The character of the landscape varies according to the lithology it is cut on; most notable is the hummocky topography and thick saprolite horizons which form over granites. Where developed on Triassic limestones, karst landforms and thick red muds are common. Strands of the Xianshuihe-Xiaojiang fault system locally disrupt the landscape and have created a number of small pull-apart basins (Fig. 1). The landscape is often gently warped down into these extensional basins (Wang, E., et al., 1998).

The rolling topography of the perched low-relief landscape contrasts sharply with the deeply incised canyons of the Red River. The Red River flows in a deep valley along the Red River fault. Most tributaries, particularly those on the Ailao Shan side of the Red River, are short, steep bedrock rivers that flow straight and approximately perpendicular to the course of the main river (Fig. 4C). Most tributaries from the northeast are short, steep bedrock rivers as well, but a few tributaries (about four) are larger with a drainage area and morphology similar to the Red River itself. Hillslopes along the main river and in the tributary valleys are steep, with frequent landslides, discontinuous soils, and sparse vegetation. Tributaries to the Red River that have their headwaters on the low-relief upland cross over one or more knickpoints, separating a low-gradient alluvial channel above from a steep bedrock channel below.

We also observe a series of broad, moderately incised valleys cut into the low-relief upland landscape, but perched above the deeply incised valleys. These broad valleys are distinct from both the low-relief upland and the deep river gorges, and we refer to them as "intermediate valleys" that together form a discontinuous intermediate landscape. Relief within these valleys (between the approximate elevation of the low-relief landscape and the knickpoint above the deeply incised valleys) is

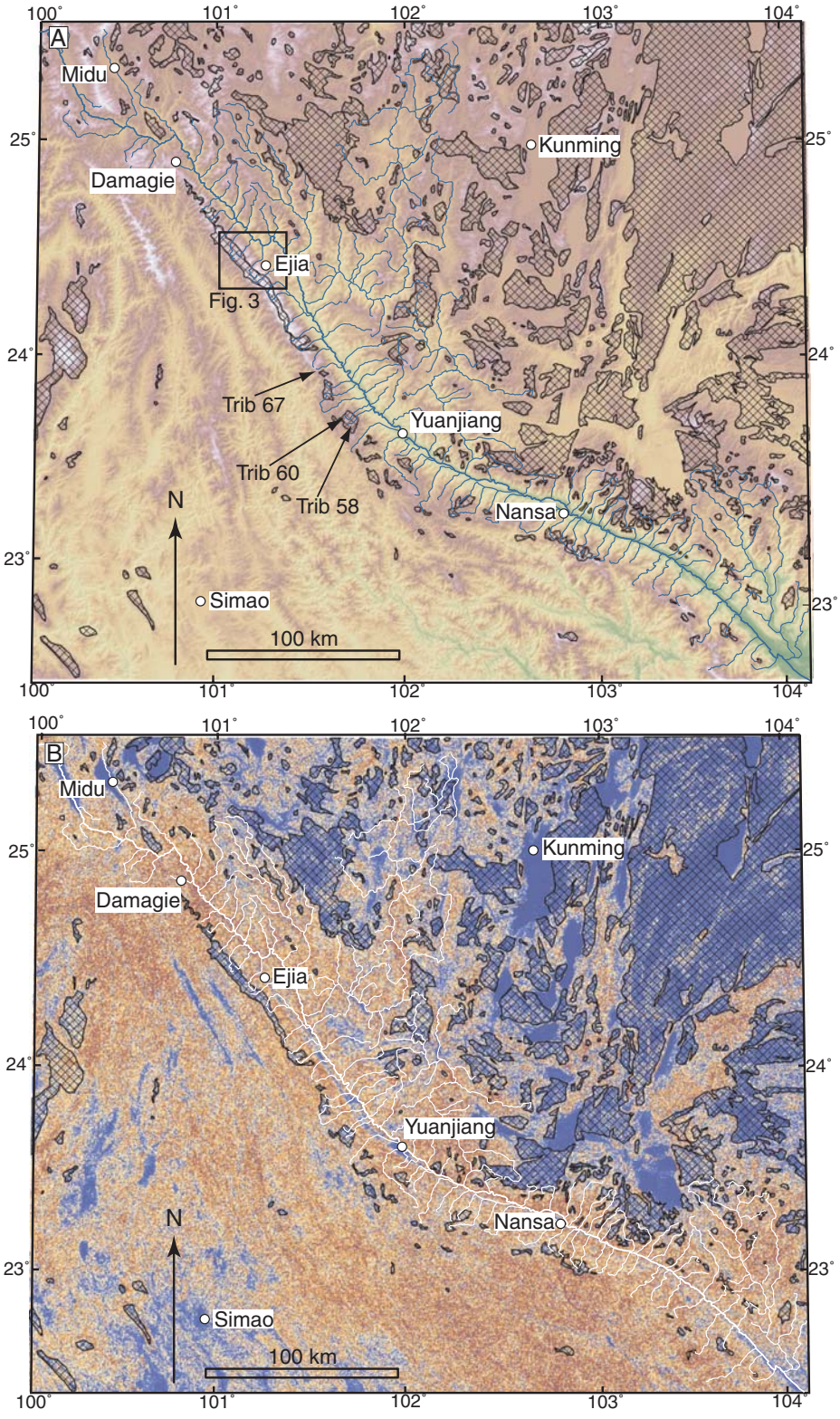

Figure 2. (A) DEM of field area. View covers same geographic area as shown in Figure 1A. The Red River drainage network is traced in blue. The Ailao Shan is the prominent range to the immediate west and southwest of the Red River. The prominent bend in the Red River fault is centered approximately at the town of Yuanjiang. The Red River fault parallels the course of the Red River and terminates in the Midu basin. The relict landscape is indicated by patterned polygons, identified by the correspondence of high elevation and low-slope areas. (B) Slope map of same area. The Red River drainage network is traced in white. Low slopes (<12°) are shown in blue, and reds and browns indicate increasing slope. The relict landscape is clearly visible as low-slope regions and is indicated by patterned polygons. Areas of low slope that do not correspond to the relict landscape are Quaternary basins along strands of the Xianshuihe-Xiaojiang fault system (see Fig. 1A) or river valley bottoms.

generally less than 1000 m. The intermediate valleys are cultivated, soils are well developed, and bedrock is deeply weathered.

In addition to field observations, we also identify the different landscape components using methods developed by Clark (2003), particularly through the combined use of topographic data, river profiles, slope and relief data, geologic maps, and CORONA areal photographs. Overlain slope and elevation maps are particularly useful for identifying low-slope areas at high elevations that correspond to the low-relief landscape, and high-slope areas at moderate to low elevations that correspond to the incised valleys (Clark, 2003). Clark (2003) finds that slopes on the low-relief landscape are generally less than ~10°, and relief is less than 600 m. We apply these methods to the Red River region, using 90-meter DEM data (see Fielding et al., 1994, for description of the data set). To the northeast of the Red River, on the Yunnan Plateau, large continuous areas of the low-relief landscape are indicated by prominent low-slope zones, although the extremely low-slope areas generally are modern depositional basins along strands of the Xianshuihe-Xiaojiang fault system (Fig. 2). To the southwest of the Red River, the low-relief landscape is clear west of Ejia (Figs. 2 and 3) and can be identified in discontinuous patches along the crest of the Ailao Shan range to the southeast. Low-slope regions both southwest of the Ailao Shan range and immediately along the Red River usually do not correspond to the low-relief landscape, but rather to valley bottoms and alluviated stretches of river (Fig. 2). Southwest of the Ailao Shan range, the low-relief, high-elevation landscape is largely absent (Fig. 2) and appears to have been removed by erosion.

MODERN, INTERMEDIATE, AND RELICT LANDSCAPES

The morphology of the southeastern margin of the Tibetan plateau, that of a deeply incised

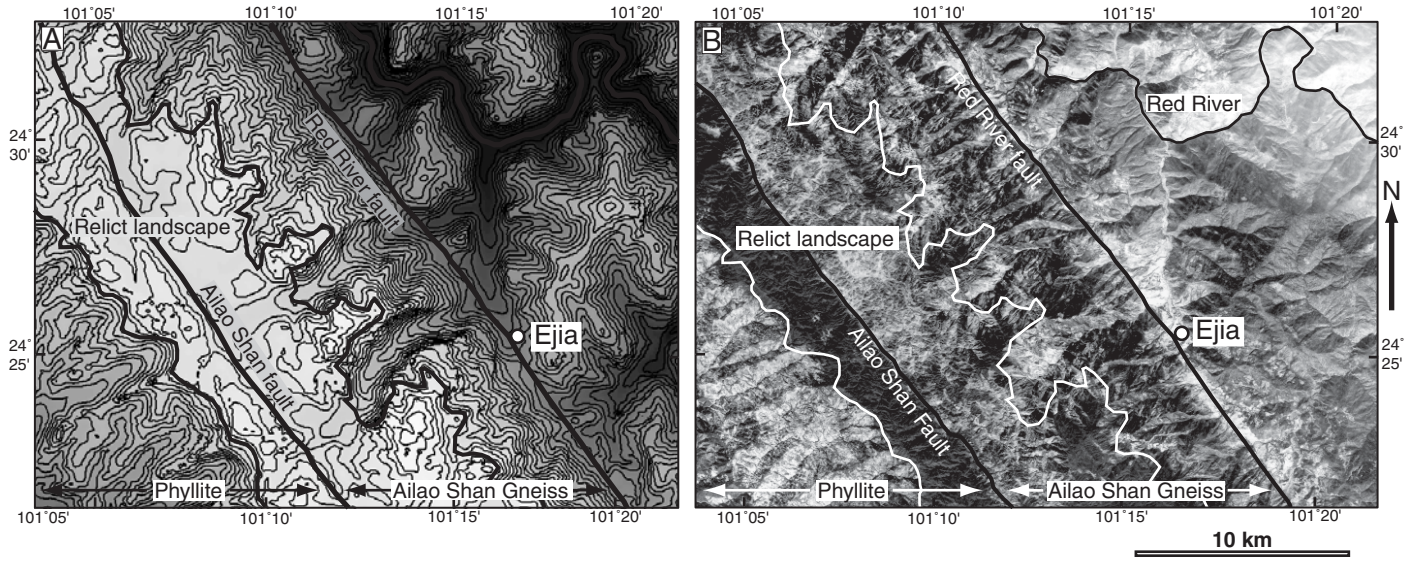

Figure 3. Relict landscape to the west of Ejia. Location indicated in Figure 2A. (A) Topographic map shaded with DEM. Also indicated are the Red River fault, Ailao Shan fault, Ailao Shan gneiss, and phyllite. The relict landscape is clearly discernible as a high, flat area and is outlined with a medium-weight line. Red River is in the upper right-hand corner. (B) CORONA aerial photographs of same area as Figure 3A. Erosion surface outlined in white. Note vegetation contrast between Ailao Shan gneiss and phyllite.

low-relief upland continuous with the Tibetan Plateau in the north and the South China coastal margin in the south, is suggestive of long-wavelength surface uplift associated with development of the Tibetan Plateau. Clark and Royden (2000) argue that this surface uplift is driven by flow of weak crustal material from beneath Tibet into adjacent regions, including the southeastern plateau margin. Injected material thickens the crust and results in isostatic surface uplift (Clark and Royden, 2000). The major rivers of the eastern margin have responded to this surface uplift through large-scale drainage reorganization (Clark et al., 2004) and by incising deep gorges (Clark, 2003).

In this interpretation, the low-relief landscape we observe in the Red River region, and which Clark (2003) observes regionally, can be used as a subhorizontal datum to track tectonic development of the region. An important component of this interpretation is that the low-relief landscape has not "regraded" to present conditions; its isolation from the incised rivers is what allows it to record surface uplift and deformation. This is consistent with several field observations in the Red River region: the deep weathering, thick saprolite, and low-gradient fluvial channels that characterize the low-relief surface suggest response to very different conditions than the incised valleys, which are characterized by exposed bedrock, landsliding, steep channels, and high relief. Low-temperature thermochronologic data elsewhere in eastern Tibet also indicate slow exhumation of an apparently correlative low-relief landscape (Kirby et al., 2002; Clark et al., 2000; Clark, 2003), and much higher exhumation rates along major tributaries to the Yangtze River (Clark et al., 2000; Clark, 2003). The low-relief landscape continues to weather, erode, and evolve, but those processes are isolated from modern base level.

In order to make clear the distinction between the base-level conditions under which these two landscape components were formed, we adopt the terms "relict landscape" (after Clark, 2003) to describe the low-relief upland landscape, and "modern landscape" to describe the incised valleys. Additionally, we employ the term "intermediate landscape" for the broad, moderately incised valleys perched above the deeply incised valleys and below the relict landscape. In our usage, "relict" refers to the conditions under which the landscape was formed and should not be taken to imply a stagnancy of the landscape. We prefer this term to the more commonly used "erosion surface," because "relict landscape" implies that a variety of geomorphic processes may have been acting on the landscape (potentially deposition as well as erosion), that the original relief structure may be complex, and that the age of formation may vary across the landscape.

One measure of the age of the relict landscape (Clark, 2003) is the age of formation of the surface, or the first time at which low-relief conditions were attained. The end of tectonic unroofing of the Ailao Shan shear zone provides an upper limit on this measure of the age of the landscape. Rapid cooling recorded by $^{40}Ar/^{39}Ar$ thermochronology between 25 and 17 Ma (Harrison et al., 1996) probably resulted from uplift and exhumation of the shear zone with correspondent high relief over the range. Cenozoic sediments preserved along the Red River to the northeast of the shear zone are coarse fluvial conglomerates derived from the Ailao Shan gneiss, and also indicate high relief within the range during this time (Wang, E., et al., 1998). Limited fission-track data from the Ailao Shan shear zone show rapid cooling between 13 and 10 Ma (Bergman et al., 1997). The relict landscape therefore is probably not older than 10 Ma and is certainly not older than 17 Ma. To the northeast on the Yunnan Plateau the landscape may have formed earlier: various parts of the relict landscape need only share the same historic base-level conditions, not the same age. Folded Eocene and rarely Oligocene units are beveled by the relict landscape in the Chuxiong basin (Fig. 1) and capped by undeformed Pliocene fossil-bearing sediments, indicating the relict landscape is younger than Eocene and older than Pliocene in this region (Wang, E., et al., 1998; Clark, 2003). Flat-lying Eocene sediments overlie folded units of the South China fold belt (Fig. 1), and therefore the relict landscape may be older than Eocene in this region (Wang, E., et al., 1998; Clark, 2003).

A second measure of the age of the relict landscape (Clark, 2003) is the age at which the river incision began and the relict landscape first became isolated from modern base level. The

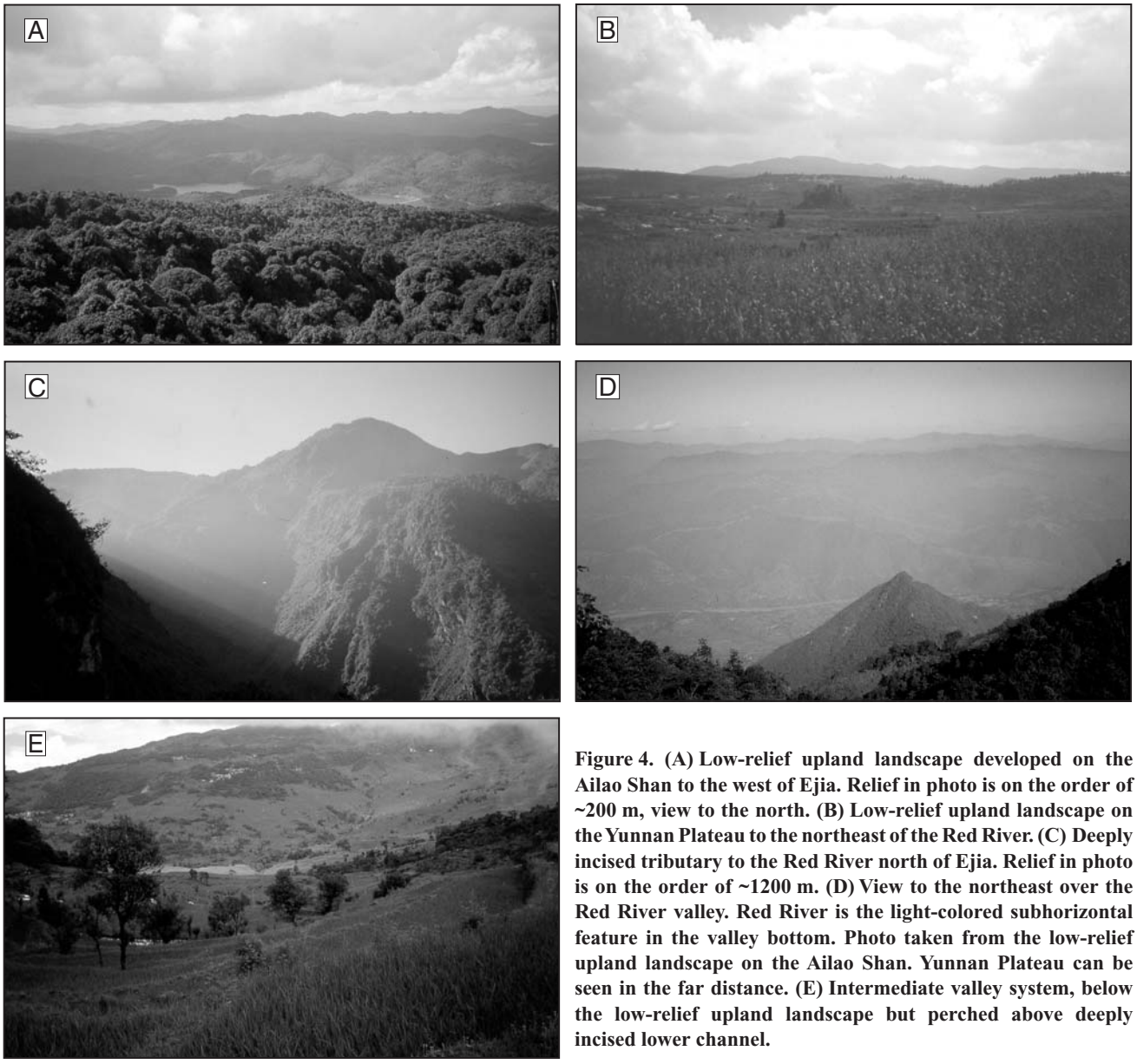

Figure 4. (A) Low-relief upland landscape developed on the Ailao Shan to the west of Ejia. Relief in photo is on the order of ~200 m, view to the north. (B) Low-relief upland landscape on the Yunnan Plateau to the northeast of the Red River. (C) Deeply incised tributary to the Red River north of Ejia. Relief in photo is on the order of ~1200 m. (D) View to the northeast over the Red River valley. Red River is the light-colored subhorizontal feature in the valley bottom. Photo taken from the low-relief upland landscape on the Ailao Shan. Yunnan Plateau can be seen in the far distance. (E) Intermediate valley system, below the low-relief upland landscape but perched above deeply incised lower channel.

timing of initiation of river incision is difficult to determine because of the paucity of well-preserved terraces within the Red River valley. However, sedimentologic evidence from near the northern termination of the Ailao Shan shear zone (Fig. 1) suggests incision in Pliocene time or later. At Damagie, fossil-bearing Pliocene sediments are deposited on the relict landscape in what appears to be the paleo–Red River valley based on the flat basal unconformity, the fluvial facies, and the slightly lower elevation (~200 m) compared to the surrounding relict landscape. These sediments are perched high above the Red River and have been incised on all sides by the main river and two tributaries. River incision must postdate deposition of these sediments and therefore can have begun no earlier than Pliocene time.

MOTIVATION: RIVER RESPONSE TO UPLIFT AND DEFORMATION

Relict landscapes (or erosion surfaces as termed by many authors) have served as important markers of tectonic uplift and deformation in a number of studies (e.g., Epis and Chapin, 1975; Gregory and Chase, 1994; Clark and Royden, 2000; Spotila and Sieh, 2000; Clark, 2003; Clark et al., 2004; for partial summaries, see Widdowson, 1997, and Phillips, 2002). However, the rivers of the southeastern margin of the Tibetan Plateau have also responded to surface uplift and deformation, and can be sensitive recorders of temporal and spatial variations in rock uplift rate (e.g., Whipple and Tucker, 1999, 2002; Snyder et al., 2000; Kirby and Whipple, 2001; Lague and Davy, 2003; Wobus et al., 2003; Whipple, 2004).

We expect the Red River and its tributaries to respond to long-wavelength surface uplift, tilting, and disruption of the relict landscape on a number of spatial and temporal scales. On the largest scale, from the headwaters of the Red River in central Yunnan to its outlet at the South China sea, the river should experience a long-wavelength tilt but a relatively stable base level set by sea level. Surface uplift and tilting should cause a steepening of the river gradient,

although channel response will also be influenced by climatic conditions. Further, although far-field base level does not change significantly, the evolution of tributaries to the Red River will depend on the "local" base level, or the elevation of the confluence of the tributary and the main river. Because tributary local base level is set by the gradient of the Red River, changes in uplift and climate conditions will be translated to the tributaries by adjustments in gradient along the main channel. It is our interpretation that each component of the landscape—the relict, intermediate, and modern—formed under different rates of local base-level fall. The modern, deeply incised lower channel segments are responding to the local modern rate of rock uplift relative to the base level set by the Red River, the intermediate landscape formed in response to an earlier local base level set by a paleo–Red River, and the relict landscape formed under stable pre-uplift base-level conditions. Therefore, both surface uplift patterns and spatial-temporal patterns of incision on the Red River (set by surface uplift, climate, and sediment and rock properties) influence the evolution of tributary channel profiles. Finally, disruptions along the active fault systems of the southeastern margin of the Tibetan Plateau can produce local variation in rock uplift rate, which will influence the morphology of local tributaries. In sum, incision along the Red River reflects regional surface uplift, tilting, climate conditions, changes in tributary local base level, and disruption along the Red River fault.

In the next section, we turn to analysis of longitudinal profiles of tributaries to the Red River, because this can be used to constrain the history of incision of the Red River. Channel parameters (such as steepness and concavity indices) can help in evaluation of the temporal and spatial sequence of incision in the Red River region: Stream-power bedrock incision modeling suggests that channel parameters should be linked to a range of external factors, including, most importantly, uplift rate and climate (Howard, 1980; Seidl and Dietrich, 1992; Howard, 1994; Whipple and Tucker, 1999, 2002). Further, a reconstructed paleo–drainage network is a basis for inferring the total amount of river incision. It can also provide a robust structural datum for measuring vertical displacement of the relict landscape across the Red River fault.

TRIBUTARY ANALYSIS

We begin with an abbreviated discussion of bedrock river incision theory, examine tributary morphology and channel parameters in the context of bedrock incision modeling, and finally, reconstruct the drainage network of the relict landscape.

Longitudinal Profile Analysis

Typical river longitudinal profiles, for both bedrock and alluvial rivers, are concave and can be described by an empirical power law relationship between slope and area:

$$S = k_s A^{-\theta}, \quad (1)$$

where S is slope, or channel gradient, k_s is the channel steepness index, A is the upstream contributing drainage area, and θ is the channel concavity index. For many landscapes, k_s varies with uplift rate, climate, and lithology, but θ varies little (Snyder et al., 2000; Kirby et al., 2003). This empirical relationship is similar to that described by the stream-power incision model for bedrock river incision (Howard, 1980; Seidl and Dietrich, 1992; Howard, 1994; Whipple and Tucker, 1999, 2002), which we briefly discuss here as a framework to guide our analysis. In the analysis we consider and discuss complexities in natural systems that may cause deviation from behavior expected for this simple model. The stream-power incision model combines a power law relationship between shear stress and erosion, conservation of mass, conditions of steady, uniform flow, and empirical relations between discharge and channel width and between discharge and basin area to arrive at the expression:

$$E = KA^m S^n, \quad (2)$$

where E is erosion rate, K is an erosion factor, a dimensional constant dependent on lithology, climate, and sediment load, and m and n are positive constants related to basin hydrology, hydraulic geometry, and erosion process. Relating channel elevation to the balance between uplift and erosion results in the expression:

$$dz/dt = U(x,t) - E(x,t) = U(x,t) - KA^m S^n, \quad (3)$$

where U is uplift rate, x is horizontal distance along the channel, and z is channel elevation. For an equilibrium channel, $dz/dt = 0$, equation 3 can be solved for equilibrium slope (S_e):

$$S_e = (U/K)^{1/n} A^{-m/n}. \quad (4)$$

Note that the form of this equation is identical to equation 1, though it applies only to bedrock (or more precisely, detachment-limited) channels. If the criteria inherent in the derivation of this model are met and a channel is in equilibrium, then the steepness index of a channel (k_s in equation 1) is a function of the ratio between uplift rate (U) and the erosion factor (K) to the $1/n$ power. There is strong empirical support for a positive correlation between the steepness index (k_s) and rock uplift rate (U) (e.g., Merrits and Vincent, 1989; Snyder et al., 2000; Kirby and Whipple, 2001; Whipple, 2004). If the U/K ratio increases uniformly along the channel, through either an increase in uplift rate or a decrease in erosivity, the channel will respond by forming a new equilibrium slope, starting at the basin outlet. The equilibration will proceed as an upstream-propagating wave of erosion (Weissel and Seidl, 1998; Whipple and Tucker, 1999). For the most part, the section upstream of this migrating "knick zone" is isolated from the change in uplift rate and will maintain a profile in equilibrium with the old uplift rate while the section downstream of the knickpoint will be equilibrated to the new conditions. The equilibration process proceeds at a rate positively correlated to drainage area, and so the trunk stream equilibrates relatively quickly, whereas headwater streams will maintain knick zones and nonequilibrated channel segments longer (Whipple and Tucker, 1999; Whipple, 2001).

The ratio m/n in equation 4, or the intrinsic concavity index, corresponds to θ, observed concavity index in equation 1, if and only if the channel is in equilibrium and rock uplift, climatic conditions, and rock properties are spatially uniform. The intrinsic concavity index should theoretically fall between 0.35 and 0.6 (Whipple and Tucker, 1999). Observed concavity indices, which may be influenced by nonuniform uplift, nonuniform lithology or variations in sediment flux and grain size (Sklar and Dietrich, 1998; Howard, 1998; Sklar and Dietrich, 2001; Whipple and Tucker, 2002; Kirby and Whipple, 2001), range from ~0.3 to 1.2 (Tucker and Whipple, 2002; Whipple, 2004). If the concavity index is significantly higher than this range, a variety of processes related to transient conditions could be in operation with important consequences (Whipple, 2004).

Tributary Morphology

Using a 90 m DEM, we extracted longitudinal profiles for 97 tributaries to the Red River in China, all those with a drainage area greater than 40 km^2 (Figs. DR1 and DR2).[1] The profiles consist of one to several channel segments separated by knickpoints, and distinct channel

[1]GSA Data Repository item 2004104, tributary longitudinal profile data and analysis details, is available on the Web at http://www.geosociety.org/pubs/ft2004.htm. Requests may also be sent to editing@geosociety.org.

parameters (see discussion in next section) can be defined for each segment. We analyzed channel segments according to their channel parameters and their position within each profile and found that tributary longitudinal profiles fall into three different morphologic categories. The dominant tributary form (78 of the 97, Figs. 5A and DR2) consists of three segments: an upper segment that travels over the relict landscape with a uniform concavity index and low steepness index, a middle segment with intermediate concavity and steepness indices, and a lower channel segment with high concavity and steepness indices (Tables 1 and DR1). For some tributaries, the upper segment is absent or poorly defined. In other cases, minor knickpoints or convex channel segments complicate segment classification. In general, however, the three-segment morphology is robust and is confirmed by our field observations of relict, intermediate, and modern landscapes described above (see Fig. 4). The second morphologic category consists of profiles with only two channel segments (four of the 97, Figs. 5B and DR2), and the final category consists of profiles that have no discernable knickpoints at all (15 of the 97, Figs. 5C and DR2). Fully equilibrated channels occur throughout the study area but are concentrated on the Yunnan Plateau in the vicinity of the bend (Fig. DR2).

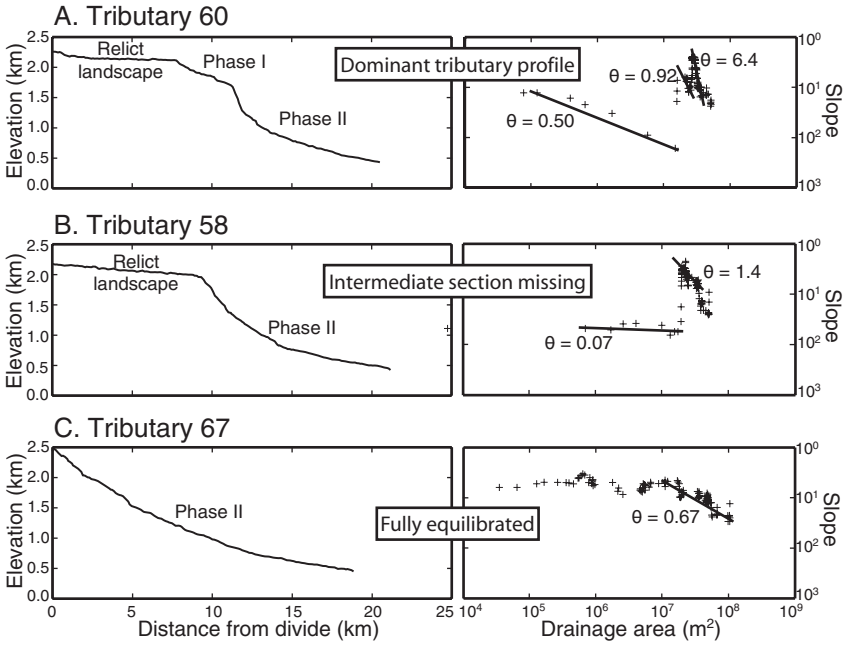

Figure 5. Longitudinal profiles and slope-area data extracted from 90 m DEM (see Fielding et al., 1994, for data set details) for three representative tributaries. Locations shown in Figure 2A. Best-fit concavity index, from equation 1, is indicated on slope-area plots. A: Tributary 60, an example of the three-segment dominant tributary form. B: Tributary 58, example in which the intermediate channel segment has been removed by headward erosion of lower segment. C: Tributary 67, an example of a fully equilibrated channel with no major knickpoints.

Channel Parameters

The intrinsic concavity index was found using methods developed by Snyder et al. (2000), Kirby and Whipple (2001), and Kirby et al. (2003). In this procedure, channel drainage area is extracted from a DEM, and corresponding slopes are calculated along the extracted channel, then these data are plotted in log-log slope-area space. A linear regression to the data yields the concavity index (the negative slope of the regression) and the steepness index (the y-intercept) (Fig. 5). Because the steepness index is highly correlated to the concavity index, a normalized steepness index was also determined for each channel with a reference concavity index (in our case, $\theta = 0.45$, though the exact value matters little, only that it is consistent for each analysis) to allow meaningful comparison of segments with different concavity indices.

In general, the concavity index and normalized steepness index for the upper and middle segments are consistent among all tributaries, and the minor variation in upper channel parameters may reflect the small sample size. In contrast lower channel segments exhibit high variability in these parameters (Table 1). Because the Red River flows directly along the Red River fault, and because we might reasonably expect

TABLE 1. NORMALIZED STEEPNESS AND CONCAVITY VALUES

Concavity†	Ailao Shan/SW	Yunnan Plateau/NE	Steepness‡	Ailao Shan/SW	Yunnan Plateau/NE
Upper Segment					
North of bend	0.42 ± 0.22 (n = 11)§	0.36 ± 0.22 (n = 6)	North of bend	32 ± 16 (n = 11)	44 ± 15 (n = 6)
South of bend	0.32 ± 0.08 (n = 5)	0.40 ± 0.18 (n = 6)	South of bend	40 ± 21 (n = 5)	29 ± 7 (n = 6)
Average	**0.38 ± 0.19** (n = 28)		Average	**35 ± 16** (n = 28)	
Middle Segment					
North of bend	0.74 ± 0.48 (n = 20)	0.56 ± 0.23 (n = 18)	North of bend	112 ± 70 (n = 20)	95 ± 37 (n = 18)
South of bend	0.51 ± 0.26 (n = 29)	0.74 ± 0.40 (n = 31)	South of bend	126 ± 53 (n = 29)	100 ± 48 (n = 31)
Average	**0.64 ± 0.37** (n = 98)		Average	**109 ± 54** (n = 98)	
Lower Segment					
North of bend	3.07 ± 1.96 (n = 22)	2.34 ± 1.96 (n = 15)	North of bend	390 ± 148 (n = 22)	220 ± 76 (n = 15)
South of bend	3.50 ± 4.36 (n = 29)	4.64 ± 3.45 (n = 27)	South of bend	277 ± 79 (n = 29)	348 ± 176 (n = 27)
Average	**3.54 ± 3.38** (n = 93)		Average	**314 ± 141** (n = 93)	
Fully Equilibrated					
North of bend	0.51 ± 0.23 (n = 2)	0.50 ± 0.14 (n = 7)	North of bend	157 ± 122 (n = 2)	129 ± 25 (n = 7)
South of bend	0.54 ± 0.21 (n = 3)	0.53 ± 0.09 (n = 3)	South of bend	159 ± 56 (n = 3)	161 ± 25 (n = 3)
Average	**0.51 ± 0.14** (n = 15)		Average	**145 ± 46** (n = 15)	

Note: Mean concavity and normalized steepness indices for upper, middle, lower, and fully equilibrated channel segments for entire drainage network (in bold) and by quadrant. Quadrants are (1) north and south of bend to the southwest of the Red River (Ailao Shan) and (2) north and south of the bend to the northeast of the Red River (Yunnan Plateau); see Figure 6C. Note increasing normalized steepness and concavity from upper to middle to lower segments, and high variability of lower segments.

†Concavity determined by linear regression to selected slope-area data using a 20 m contour interval.

‡Normalized steepness index determined by linear regression to slope-area data with a fixed concavity of 0.45.

§Number of tributaries used in average. In some cases, more than one middle or lower channel segment can be identified in each tributary, separated by knickpoints and with slightly different steepness and concavity. Channel parameters for each segment were retained and used to determine mean values. This results, in some cases, in a greater number of channel segments than there are actual channels.

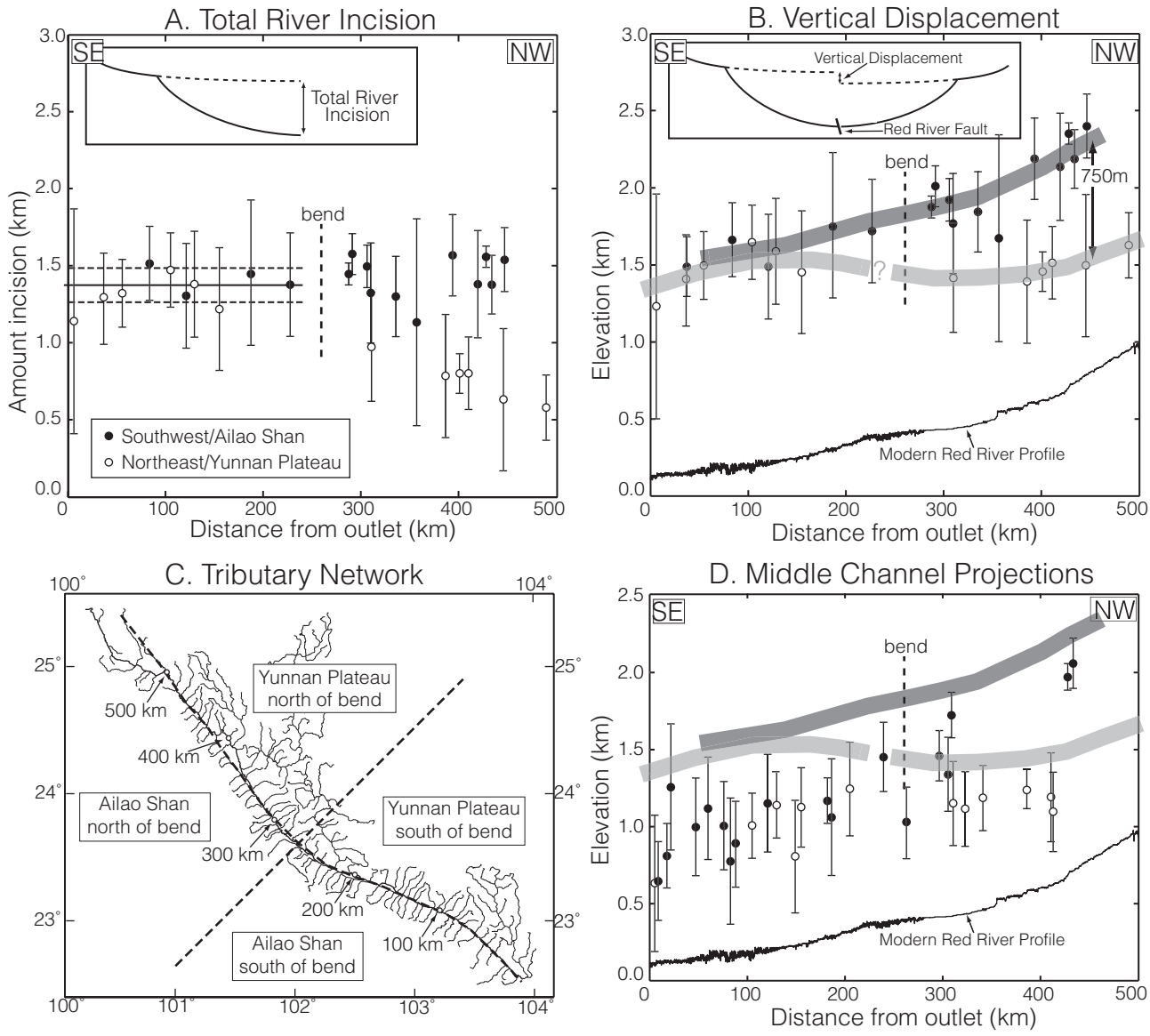

Figure 6. Projected channel segment data plotted against distance from the basin outlet near the Chinese-Vietnamese border, with the bend at ~260 km upstream from basin outlet. A: River incision, calculated by projecting upper segments and subtracting modern river elevations (see inset). Regression of data south of bend shown at 1381 ± 88 m. B: Projected upper-segment elevations. Interpreted vertical displacement across the Red River fault (see inset) shown by thick lines. A maximum vertical displacement of ~750 m is recorded. Longitudinal profile of Red River also shown. C: Approximate distances upstream from outlet and location of bend shown in relation to the Red River tributary network. D: Projected middle-segment elevations. Upper-segment displacement lines and Red River longitudinal profile shown, same as for Figure 6B. Incision is approximately two times greater from the middle to lower segments than from the upper to middle segments.

different deformation patterns north and south of the major bend, we present averaged data for each set of segments as well as averaged data for the four quadrants defined by the river and the bend (Fig. 6). We also present data for the 15 tributaries with no knickpoints, which we label as "fully equilibrated" in Table 1.

A number of observations emerge from these data. First, there is only minor geographic variation in normalized steepness and concavity index data for the upper and middle channel segments, which contrasts with significant variability in the lower channel segments. Second, the average normalized steepness index increases from the upper channel segments to the middle to the lower segments. Finally, the average concavity index for the upper landscape segments (0.38 ± 0.19) falls within the range of commonly observed values (Tucker and Whipple, 2002), and average concavity index for middle channel segments (0.64 ± 0.37) is higher but is still within the normally observed range. Lower-segment concavity indices, however, are exceptionally high (3.54 ± 3.38).

Reconstruction of Relict Landscape Channel Profiles

Of the 97 total tributary longitudinal profiles, we identified well-developed "relict landscape"

channel segments on 50 tributaries on the basis of low normalized steepness index, average concavity index values, and their position above a prominent knickpoint. Each of these segments was evaluated for conditions that might affect channel gradient or knick zone propagation, particularly lithologic contrasts along the length of each channel. Such segments were excluded, as were segments with insufficient data to obtain a meaningful regression. Our final, conservative data set includes 12 tributaries from the Yunnan Plateau northeast of the Red River and 16 from the southwest, draining the Ailao Shan range (Fig. DR3; Table DR2; see footnote 1).

The properties of these 28 channels were analyzed to estimate the preincision profiles to their confluence with the Red River. The mean concavity index (θ) for the upper channel segments is 0.38 (Table 1). Using this value, drainage area and slope data, and equation 1, we obtained a steepness index (k_s) and uncertainty for each segment. From these values, we then projected the channel profile from the knickpoint downstream to the Red River confluence. This analysis provides an estimate of the paleo–longitudinal profile of each tributary corresponding to the drainage network developed on the relict landscape, assuming no changes in drainage area. Because we use equation 1, our analysis does not depend on the validity of bedrock incision modeling, but rather only on well-established empirical observation of a power law relation between local slope and upstream drainage area.

The difference in elevation of the termination of the profile and that of the modern tributary–Red River confluence indicates the amount of subsequent incision: The reconstructed longitudinal profiles indicate 500–1600 m of incision (Fig. 6A). The difference in elevation of the termination of the profile between tributaries from the Ailao Shan range and from the Yunnan Plateau indicate the relative vertical displacement of the relict landscape by the Red River fault (Fig. 6B). Southeast of the bend in the Red River fault, tributaries from the Ailao Shan range and Yunnan Plateau project to approximately the same elevation, indicating only minor if any offset across the fault. To the northwest of the bend, however, displacement increases to a maximum of 750 m. Insufficient data in the vicinity of the bend hinder precise estimation of the offset in that area. Although tributary data do not extend to the northern tip of the Red River fault, field observations indicate that vertical displacement must diminish toward the Midu basin as well (Fig. 1).

We also reconstructed the middle channel segment longitudinal profiles for 14 of the 28 tributaries with upper segments, and for 16 additional channel profiles with no upper segments, for a total of 30 projections (Figs. 6C and DR3; Table DR2; see footnote 1). We used a concavity index of 0.64 (mean for middle segments, Table 1). Data for tributaries with both upper- and middle-segment projections allow us to constrain the relative amount of river incision recorded by base-level fall from the relict landscape channel to the middle segment, and from the middle segment to the modern river elevation (Table 2). Though the sparseness of these data limits inferences, approximately twice as much incision occurred from the middle to lower channel segments as from the relict landscape to middle channel segments, and appears to be greater north of the bend.

TABLE 2. PHASE II to PHASE I INCISION RATIO

	Ailao Shan/SW	Yunnan Plateau/NE
North of bend	3.0 ± 0.2 (n = 4)†	2.8 ± 0.5 (n = 3)
South of bend	1.1 ± 0.3 (n = 3)	1.6 ± 0.2 (n = 4)
Average	2.3 ± 0.1 (n = 14)	

Note: Incision during each phase determined by fitting upper and middle channel segments using a concavity of 0.38 and 0.64, respectively (Table 1), projecting the channels to their intersection with the paleo–Red River, then subtracting modern river elevations.
†Number of tributaries used in average.

DISCUSSION

Key observations that emerge from our tributary analysis are (1) total amount and distribution of incision along the Red River (Fig. 6A), (2) a three-segment channel morphology for the majority of tributaries (Figs. 5 and DR2), (3) high mean concavity index (θ) for the lowermost channel segments (Tables 1 and DR1), (4) the relative offset of relict landscape tributaries across the Red River fault (Fig. 6B), and (5) geographic variation in normalized steepness index (k_s) and concavity index (θ) for the lowermost channel segments (Table 1). The latter two factors yield information about activity along the Red River fault and will be addressed in the first section of the discussion. The first three factors relate to surface uplift and climatic interactions and will be addressed in a later section. Finally, we will discuss implications of our observations for exhumation of the Ailao Shan shear zone and for growth of the eastern margin of the Tibetan Plateau.

Activity along the Red River Fault

The Red River fault is clearly an active strike-slip fault, although previous workers have not been able to determine the magnitude of strike-slip or dip-slip displacement, spatial distribution, or timing with certainty (Allen et al., 1984; Wang, E., et al., 1998; Replumaz et al., 2001). Because the topographic relief of the relict landscape is significant relative to the amount of displacement we expect across the Red River fault, and as there may have been remnant relief along the crest of the Ailao Shan range, topography alone is an insufficient datum for measuring vertical displacement. Using instead the reconstructed drainage network mitigates these problems and allows us to place constraints on vertical displacement.

The longitudinal profiles of two directly opposing tributaries may have different concavity or steepness indices, but their downstream elevations must be the same, set by the elevation of the main channel (Seidl and Dietrich, 1992). Once river incision begins, the upper portions of the opposing tributaries are isolated from each other and begin to record any differential offset occurring downstream of the knickpoint (see Fig. 6B inset). Reconstruction of relict landscape tributaries reveals that Ailao Shan range tributaries are displaced vertically relative to Yunnan Plateau tributaries. Relative displacement is insignificant south of the bend but increases toward the north to a maximum displacement of ~750 m near the town of Ejia (Fig. 6B). Absolute displacement may have occurred in the footwall (increasing the surface elevation of the Ailao Shan range), in the hanging wall (downwarping the Yunnan Plateau), or both.

The mean normalized steepness index (k_s) in the lowest channel segments varies considerably by geographic region (Table 1): Channels are steepest north of the bend in the Ailao Shan range and south of the bend on the Yunnan Plateau (390 ± 148 and 348 ± 176, respectively), and are less steep south of the bend in the Ailao Shan range and north of the bend on the Yunnan Plateau (277 ± 79 and 220 ± 76, respectively) (Fig. 1). The steepness index in these channels varies as a function of lithology and rate of relative base-level fall. Within the Ailao Shan shear zone, lithology is uniform. Therefore, variations in channel steepness index probably reflect different uplift conditions: In the northern Ailao Shan range, where uplift rate (and relative base-level fall) is higher as a result of dip-slip displacement on the Red River fault, steepness indices are correspondingly higher (equation 4; Table 1). Lower steepness indices north of the bend on the Yunnan Plateau may similarly result from downwarping of the hanging wall by vertical displacement on the Red River fault, and downwarping may also be responsible for the high concentration of fully equilibrated channels on the Yunnan Plateau on either side of the bend near Yuanjiang (Fig. DR2). However, this analysis is complicated by lithologic

differences north and south of the bend, which probably play an important role in determining the channel steepness index. Many of the tributaries from the Yunnan Plateau south of the bend drain cliff-forming Triassic limestones of the southern South China fold belt (Fig. 1), capable of supporting extremely steep channels. Farther north, where tributaries drain the relatively erodible sediments of the Chuxiong red bed basin (Fig. 1), channel steepness indices are lower. Why the effect of lithology is not seen in the middle and relict landscape channel segments is unclear. One possibility is that the relict landscape and middle channel segments are in transport-limited rather than detachment-limited (bedrock) conditions, and therefore, lithologic controls on channel morphology are masked (Whipple and Tucker, 2002).

The maximum gradient associated with regional tilting, which will affect tributary data, is ~2×10^{-3} (5000 m over 2500 km, Clark and Royden, 2000). However, because tilting is stronger near the plateau and gentler in more distal positions (Clark and Royden, 2000), because we do not know the original landscape gradient, and because the Red River runs slightly oblique to the plateau axis, tilting in the study area is probably less. On this basis, and from DEM analysis, we estimate tilting was on the order of 1×10^{-3}. Over the 500 km of the study area, if we use this value, surface uplift at the northwest end of the study area is ~500 m greater than at the southwest end. This tilting does not affect relative displacement across the Red River fault, but does affect the paleo–Red River profile recorded by tributaries from the Ailao Shan range and Yunnan Plateau. The gradient recorded by the Yunnan Plateau tributaries is ~2×10^{-4}, less than our estimated tilting gradient. This is probably the result of downwarping of tributaries northwest of the bend along the Red River fault. The higher gradient recorded by Ailao Shan tributaries (~2×10^{-3}) may similarly result from relative uplift of the footwall along the Red River fault.

In summary, the dip-slip component of displacement along the Red River fault is less than 750 m north of the bend and insignificant south of the bend, affecting both hanging-wall and footwall elevations. This is not consistent with models for the Red River fault in which displacement extends along the entire length of the fault (Allen et al., 1984; Replumaz et al., 2001). Further, a number of authors have suggested that significant unroofing of the Ailao Shan shear zone has occurred as a result of recent normal faulting along the Red River fault (Harrison et al., 1996; Leloup et al., 2001; Replumaz et al., 2001). Our tributary data and observations of landscape morphology indicate conclusively that no exhumation of the shear zone has occurred since establishment of the relict landscape, probably prior to Pliocene time.

River Incision and Surface Uplift

The existence of a regional relict landscape at high elevations, which is continuous with the Tibetan Plateau, implies significant surface uplift of the southeastern plateau margin (Clark et al., 2002; Clark, 2003). We discuss incision along the Red River in the context of this regional uplift below.

Incision and Surface Uplift Recorded by the Red River

The Red River has incised the landscape between ~500 and ~1600 m (Fig. 6A), though tributaries on the Yunnan Plateau record less incision. Because absolute elevations on both the Ailao Shan range and the Yunnan Plateau north of the bend have probably been affected by differential vertical displacement on the Red River fault, we cannot use the river incision recorded by these tributaries as a proxy for total river incision. South of the bend, however, tributaries on either side of the Red River are relatively unaffected by recent faulting, and these data indicate a weighted mean river incision of 1381 ± 88 m (Fig. 6A). Maximum surface uplift at the southern end of the study area is indicated by the current approximate elevation of the projected tributaries, or ~1500 m (Fig. 6B). Prior to surface uplift, the paleo–Red River was probably at a similar or lower elevation (<100 m) to the modern Red River, but the paleo–Red River profile has been translated through surface uplift to its current elevation of ~1500 m (Fig. 6B). Surface uplift at this point is therefore 1400–1500 m (the amount of uplift necessary to elevate the paleo–Red River profile from 0 m (the minimum original profile elevation) or ~100 m (the maximum original profile elevation) to ~1500 m (the approximate elevation today). Total surface uplift must increase upstream toward Tibet.

Incision and Surface Uplift Recorded by Tributaries to the Red River

Multiple-segment tributary longitudinal profiles (Figs. 5 and DR2) indicate a complicated incision pattern. Knickpoints can result from a variety of processes, which we will explore below. However, it is unlikely that the knickpoints in this study result from river capture events. Clark et al. (2004) argue that prior to regional uplift, most of the major rivers of eastern Tibet, including the Mekong, Salween, Yangtze, and tributaries to the Yangtze, drained through the Red River to the South China Sea. The modern drainage pattern is a result of river captures driven by uplift of the southeastern margin. However, the morphology of the Yangtze and other rivers (Clark et al., 2004) suggests that these captures occurred immediately prior to regional uplift and river incision, and therefore excavation of the Red River valley was accomplished exclusively by the Red River, regardless of its prior drainage history. Knickpoints within the Red River basin are therefore most likely unrelated to large-scale drainage reorganization.

In a detachment-limited bedrock river, knickpoints can also result from a change in uplift rate (U) or other conditions such as precipitation or erosion mechanism (K) (equation 4). An increase in uplift rate initiates the migration up the profile of a steep channel segment, separated from the upstream segments by a knickpoint (Weissel and Seidl, 1998; Whipple and Tucker, 1999). The steepness index of the newly forming channel segment will depend on the term $(U/K)^{1/n}$ from equation 4. Sudden base-level fall can also produce migrating knickpoints, but channel segments above and below the knickpoint will have the same steepness and concavity indices, assuming the background rate of base-level fall is unchanged (Whipple and Tucker, 1999).

The three-segment tributary morphology (Fig. 5A) is thus most simply interpreted as pulsed surface uplift (Fig. 7A): During the first phase of incision, uplift rate increased, isolating the upper, relict landscape channel and developing the intermediate channel with higher mean normalized steepness index (Table 1); during the second phase of incision, uplift rate increased further, isolating the intermediate channel and initiating the modern, lower channel segment with yet higher mean normalized steepness index (Table 1). We can make this interpretation, however, only if tributary local base level remains constant throughout development of the region; that is, if the Red River maintains a relatively constant gradient during uplift. Even though the Red River is constantly incising, if the gradient is stable, absolute base level for each tributary will be constant in time, and changes in uplift rate will be directly translated to the tributaries.

However, it is unlikely that the main Red River profile is unaffected by regional uplift and climate change. The trunk river has considerable latitude in adjusting to changes in external conditions, including possible changes in channel width, sinuosity, percent alluvial cover, bed material size, bed roughness, and gradient. A crucial factor in determining the evolution of tributary longitudinal profiles, therefore, is the nature of the response of the main river to changes in uplift rate (U) and climate and erosion conditions (related to K).

If surface uplift rate has been constant during river incision, we may infer changes in gradient of the Red River on the basis of tributary morphology. Local base-level change brought about by changing absolute elevation along the trunk channel effectively enhances or detracts from the regional uplift rate. The following scenario would produce three-segment channels (Fig. 7B). As uplift rate first increased, the Red River steepened, increasing absolute elevation at every point along the channel. During this period, the effects of increased uplift rate on channel steepness were dampened by rising local base level on the trunk channel. Following this, climate change, possibly a shift in the Quaternary to more erosive conditions (Gregory and Chase, 1994; Molnar, 2001), or a surface uplift–induced intensification of the monsoon (Ruddiman and Kutzbach, 1989) triggered downcutting of the main channel and the establishment of the new profile at lower absolute elevations. Base-level fall initiated the lower channel segments and enhanced the effect of regional surface uplift, resulting in very steep channels.

Incision history may also be reflected in the high concavity index of the lower channel segments, which have a mean value of 3.54 ± 3.38, compared to middle-segment values of 0.64 ± 0.37 and upper-segment values of 0.38 ± 0.19 (Table 1). The effects of transient adjustment, alluviation near the tributary junction with the main river, data noise, lithology, sediment supply (Sklar and Dietrich, 1998; Howard, 1998; Sklar and Dietrich, 2001; Whipple and Tucker, 2002), bed armoring (Seidl et al., 1994), other spatially correlated effects (Kirby and Whipple, 2001; Kirby et al., 2003), or a transient response to rapid base-level fall (Gasparini, 2004) could increase observed channel concavities, and may account for increases in the concavity index of the order observed in the lower tributary segments. However, temporal variations in uplift rate can also affect the concavity index of a channel by producing a series of equilibrium channel segments that sweep up the profile in succession (Royden et al., 2000; Whipple and Tucker, 1999). If uplift rate decreases with time, channel segments formed earlier, during higher-uplift conditions, in the upper parts of the channel, will be steeper. Later-formed channel segments, near the tributary outlet will be less steep. If the decrease in uplift rate is smooth, the result will appear as a highly concave channel profile. High lower-channel-segment concavity index (Table 1) suggests declining uplift rate with time during the second phase of incision (Fig. 7A). Alternatively, incision along the trunk channel during the second phase of incision may initially have been rapid, during the period of base-level fall, but has fallen to more moderate values toward the present (Fig. 7B).

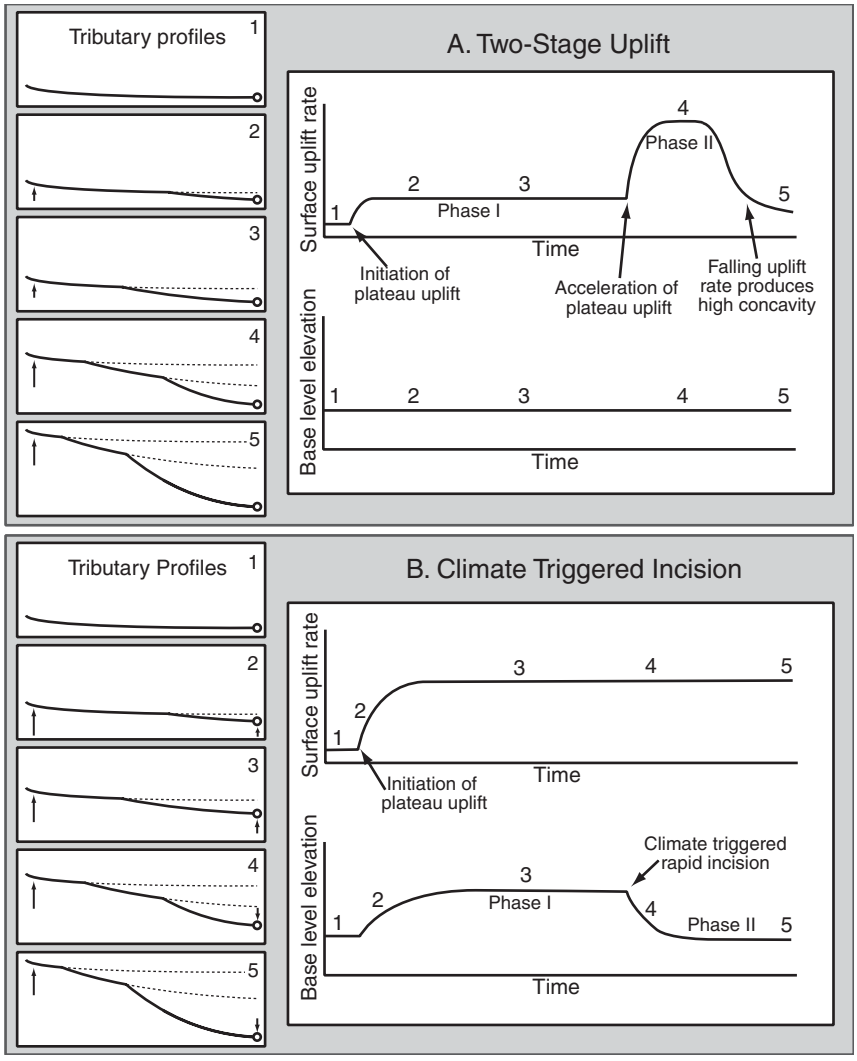

Figure 7. End-member scenarios resulting in two-phase incision. Time slices shown on left with numbers corresponding to positions along time axis on graphs on right. A: Two-phase uplift history. In this scenario, tributary base level (therefore the profile of the main channel) is constant with time. Pulses in plateau growth are directly translated to tributary morphology. B: Constant uplift rate with climate interactions. In this scenario, the main channel adjusts to plateau uplift by changing its gradient and therefore increasing local tributary base level (times 2 and 3). Rapid river incision is triggered, likely by climatic conditions, and the main channel returns to a lower gradient, causing tributary base-level fall (times 4 and 5). Base-level changes, against a background of constant uplift, result in the two-phase river incision.

In summary, we assign the upper knickpoints and abandonment of the relict landscape to rapid onset of uplift-driven river incision. Two end-member scenarios emerge for subsequent development of the Red River basin, one in which tributary morphology is entirely driven by changes in uplift rate with time, the other in which uplift rate is constant in time, and tributary morphology is the result of adjustments of the trunk channel to external forcings such as climate factors. We know of no geodynamic reason why plateau growth might be pulsed, but the possibility is certainly intriguing and worth further investigation. We do, however, strongly suspect that climate change over the duration of river incision is important. Short-term climate fluctuations would likely damp out over the duration of development of the Red River drainage. However, global climate and monsoonal patterns and intensity do vary over longer time scales, and monsoon intensity may have been enhanced by the uplift

of the plateau surface (Ruddiman and Kutzbach, 1989). Although the quantitative relation between climate and river erosivity is not well known, increased flood discharges associated with an intensification of the monsoon ought to enhance river incision rates and importantly influence landscape evolution in the region.

As an interesting side note, channels with fewer channel segments (Figs. 5A and 5B) may result from variable rates of knickpoint migration. If the knickpoint separating the middle and lower segments migrates quickly up the channel, it may overtake the upstream knickpoint separating the upper and middle segments, erasing the middle segment entirely from the profile (Fig. 5B). It may also migrate beyond the uppermost knickpoint, overtaking both the middle and upper segments (Fig. 5C). Knickpoint migration rate, in the stream-power bedrock incision model, is sensitive to U, K, and n (equation 4; Whipple and Tucker, 1999; Weissel and Seidl, 1998; Royden et al., 2000). As the three tributaries shown in Figure 5 are closely spaced within the relatively uniform gneisses of the Ailao Shan shear zone, to a first order we would expect very similar values of U, K, and n for each tributary, and therefore expect tributary morphology to be nearly identical. That this is not the case underlines the sensitivity of knickpoint migration to what we suspect are only small variations in factors that control erosion parameters.

Exhumation of the Ailao Shan Shear Zone

Development of an extensive, low-relief landscape indicates that a period of regional erosion and relief reduction followed exhumation of the shear zone. During its exhumation, the Ailao Shan was a high range, shedding debris into a fluvial system along its northeastern edge (Wang, E., et al., 1998). The high relief within the Ailao Shan shear zone during its unroofing phases was reduced to low relief and was deeply weathered by the time river incision began in the Pliocene or later. However, because the shape of the modern Red River basin is inherited from the relict landscape, and because the Ailao Shan range is a modern drainage divide, it must have remained a subtle topographic high even after reduction to low relief.

While the Ailao Shan range has experienced surface uplift since formation of the relict landscape, the preservation of the relict landscape indicates that the shear zone has not been structurally or erosionally exhumed. We cannot assess the role of a possible paleo–Red River fault in exhumation of the Ailao Shan shear zone prior to formation of the relict landscape, but we have demonstrated that dip-slip displacement along the modern Red River fault plays no role in exhumation of the shear zone, counter to the findings of several other workers (Leloup et al., 1995, 2001; Harrison et al., 1996; Gilley et al., 2003). Additionally, river incision is not extensive enough to have reset low-temperature thermochronometers as it has elsewhere on the eastern margin of the Tibetan Plateau (Xu and Kamp, 2000; Clark and Royden, 2000; Kirby et al., 2002). Therefore, all thermochronologic data showing rapid cooling relate to earlier, pre–relict landscape exhumational events. In particular, fission-track data (Bergman et al., 1997), which indicate rapid cooling at ca. 10 Ma, cannot be linked to initiation of normal faulting on the modern Red River fault as it is by Leloup et al. (2001).

Plateau Growth

In the Red River region, river incision in the Pliocene or later probably closely followed the initiation of growth of the eastern margin of the Tibetan Plateau. Plateau growth may have been in two phases, based on the three-segment tributary morphology, but this may also be the result of factors such as climate change in Quaternary time. Total surface uplift near the Chinese-Vietnamese border at the southern end of the study area is 1400–1500 m. The paleo–Red River defines the base of the relict landscape, but relief within the relict landscape is up to 500 m, and average elevation of the relict at the southeast end of the study area is ~1800 m. Subtracting from this the amount of surface uplift, average elevations were probably only a few hundred meters above sea level prior to surface uplift.

Pliocene initiation of incision in the Red River region is somewhat later than the initiation of river incision inferred from thermochronologic data from elsewhere along the plateau margin. Kirby et al. (2002) infer uplift of the plateau adjacent to the Sichuan basin in late Miocene or early Pliocene time (10–12 Ma in the Longmen Shan, west edge of Sichuan basin, and 5–7 Ma in the Min Shan, north edge of Sichuan basin) on the basis of rapid cooling recorded in (U-Th)/He and $^{40}Ar/^{39}Ar$ data. Rapid river incision in late Miocene time (7–13 Ma) is implied by the apatite (U-Th)/He data of Clark (2003). The Red River region is farther southeast along the plateau margin from Tibet than these other study areas (see Fig. 1), and thus probably experienced less overall surface uplift, and that uplift may have occurred more recently. A delay in the initiation of incision along the Red River compared to regions proximal to Tibet suggests outward growth of the Plateau.

CONCLUSIONS

We describe a low-relief upland landscape in the areas adjacent to the Red River in Yunnan Province, China, continuous with a landscape developed over the entire eastern margin of the Tibetan Plateau (Clark et al., 2002, 2004; Clark, 2003), which we interpret as a relict landscape: a landscape with a morphology that reflects past rather than present base-level conditions. The relict landscape is cut by the active fault systems of Yunnan, including the Red River fault, and it is deeply incised by the Red River. Tributaries to the Red River record incision and tectonic deformation of the region, including ~1400 m river incision, ~1400–1500 m surface uplift, up to 750 m dip-slip offset across the northern portion of the Red River fault, and two phases of river incision.

The following history for structural and geomorphic development of the region emerges. The Ailao Shan shear zone was active, and actively unroofing, until at least 17 Ma (Harrison et al., 1996) and possibly as recently as 10 Ma (Bergman et al., 1997; Leloup et al., 2001). After that time, deep weathering and erosion reduced the area to low relief (<500 m) and low average elevation, sharing base level with the regional low-relief landscape identified by Clark (2003). At some point, possibly in Pliocene time, the area began to undergo regional uplift and tilting, and the Red River responded by incising a deep valley into the now elevated low-relief landscape, forming the relict landscape. Regional uplift is almost certainly related to uplift of the Tibetan Plateau, and a plausible mechanism has been suggested by Royden (1996), Royden et al. (1997), and Clark and Royden (2000), in which the extrusion of weak lower crustal material from beneath Tibet causes the inflation and uplift of the eastern margin of the Tibetan Plateau.

Structural deformation produced at most 750 m of uplift of the northern Ailao Shan range, tapering toward zero south of the bend and at the northern termination of the fault in the Midu basin. The relict landscape has not been erosionally or structurally removed from the Ailao Shan shear zone, and therefore no unroofing of the shear zone has occurred along the Red River fault or any other structure since the formation of the relict landscape.

The spatial and temporal pattern of river incision reflects both regional uplift and climate conditions. The tributary three-segment morphology could indicate two phases of plateau growth: relatively slow growth during the first phase, then a pulse of rapid uplift during the second phase. More likely, however, the two-phase incision history results from adjustments

of the trunk channel to changing conditions of uplift and climate. The trunk channel may have initially increased in gradient as a response to regional uplift, then rapidly cut down to a new equilibrium profile after a trigger to more erosive conditions, such as climate change in the Quaternary or monsoonal strengthening. While we cannot rule out the intriguing possibility of pulsed plateau growth, we acknowledge that climatic conditions almost certainly will play a role in the development of any river system of this size and over this length of time.

ACKNOWLEDGMENTS

This research was supported by the Continental Dynamics program at the National Science Foundation (EAR-0003571). We thank Marin Clark and Wiki Royden for helpful discussion of this work; Sinan Akciz, Will Ouimet, and Christopher Studnicki-Gizbert for discussion and manuscript reviews; Michael Stewart, Josh Feinberg, and Yin Jiyun for invaluable assistance in the field; and driver Kou Jianle for five safe field seasons. This paper benefited from thorough reviews by F. Pazzaglia and J. O'Connor.

REFERENCES CITED

Allen, C.R., Gillespie, A.R., Han, Y., Sieh, K.E., Zhang, B., and Zhu C., 1984, Red River and associated faults, Yunnan Province, China: Quaternary geology, slip rates, and seismic hazard: Geological Society of America Bulletin, v. 95, p. 686–700.

Bergman, S.C., Leloup, P.H., Tapponnier, P., Schärer, U., and O'Sullivan, P., 1997, Apatite fission track thermal history of the Ailao Shan–Red River shear zone, China: Strasbourg, France, paper presented at meeting, European Union of Geoscience, 1 p.

Brias, A., Patriat, P., and Tapponnier, P., 1993, Updated interpretation of magnetic anomalies and seafloor spreading stages in the South China Sea, implications for the Tertiary tectonics of SE Asia: Journal of Geophysical Research, v. 98, no. B4, p. 6299–6328.

Bureau of Geology and Mineral Resources of Yunnan Province, 1990, *in* Regional Geology of Yunnan Province: Beijing, Geological Publishing House, 728 p.

Clark, M.K., 2003, Late Cenozoic uplift of southeastern Tibet [Ph.D. thesis]: Cambridge, Massachusetts Institute of Technology, 226 p.

Clark, M.K., and Royden, L.H., 2000, Topographic ooze: Building the eastern margin of Tibet by lower crustal flow: Geology, v. 28, p. 703–706.

Clark, M.K., House, M., Royden, L.H., Burchfiel, B.C., Zhang, X, Tang, W., and Chen, Z., 2000, River incision and tectonic uplift in eastern Tibet from low-temperature apatite U-Th/He thermochronology: Eos (Transactions, American Geophysical Union), Fall Meeting Supplement, v. 81, p. F1142.

Clark, M.K., Royden, L.H., Burchfiel, B.C., Whipple, K.X, House, M.A., and Zhang, X., 2002, Preservation of a low-relief, regionally continuous erosion surface in southeastern Tibet: Evidence for the transient condition of the southeastern plateau margin: Geological Society of America Abstracts with Programs, v. 34, no. 6, p. 411.

Clark, M.K., Schoenbohm, L.M., Royden, L.H., Whipple, K.X, Burchfiel, B.C., Zhang, X., Tang, W., Wang, E., and Chen, L., 2004, Surface uplift, tectonics, and erosion of eastern Tibet from large-scale drainage patterns: Tectonics, v. 23, TC1006, doi:10.1029/2002TC001402.

Cobbold, P.R., and Davy, P., 1988, Indentation tectonics in nature and experiment 2, Central Asia: Uppsala, Sweden, Geological Institute, University of Uppsala, v. 14, p. 143–162.

Davy, P., and Cobbold, P.R., 1988, Indentation tectonics in nature and experiment 1, Experiments scaled for gravity: Uppsala, Sweden, Geological Institute, University of Uppsala, v. 14, p. 129–141.

Dewey, J., Cande, S., and Pitman, W.C., III, 1989, Tectonic evolution of the India-Eurasia collision zone: Eclogae Geologicae Helvetiae, v. 82, p. 717–734.

Epis, R.C., and Chapin, C.E., 1975, Geomorphic and tectonic implications of the post-Laramide Late Eocene erosion surface in the Southern Rocky Mountains: Geological Society of America Memoir 144, p. 45–74.

Fielding, E., Isacks, B., Barazangi, M., and Duncan, C., 1994, How flat is Tibet?: Geology, v. 22, p. 163–167.

Gasparini, N.M., Tucker, G.E., and Bras, R.L., 2004, Network-scale dynamics of grain-size sorting: Implications for downstream fining, stream-profile concavity, and drainage basin morphology: Earth Surface Processes and Landforms (in press).

Gilley, L.D., Harrison, T.M., Leloup, P.H., Ryerson, F.J., Lovera, O.M., and Wang J.H., 2003, Direct dating of left-lateral deformation along the Red River shear zone, China and Vietnam: Journal of Geophysical Research, v. 103, no. B2, 2127, doi:10.1029/2001JB001726.

Gregory, K.M., and Chase, C.B., 1994, Tectonic and climatic significance of a late Eocene low-relief high-level geomorphic surface, Colorado: Journal of Geophysical Research, v. 99, no. B10, p. 20,141–20,160.

Hallet, B., and Molnar, P., 2001, Distorted drainage basins as markers of crustal strain east of the Himalaya: Journal of Geophysical Research, v. 106, no. B7, p. 13,697–13,709.

Harrison, T.M., Chen, W., Leloup, P.H., Ryerson, F.J., and Tapponnier, P., 1992, An early Miocene transition in deformation regime within the Red River fault zone, Yunnan, and its significance for the Indo-Asian tectonics: Journal of Geophysical Research, v. 97, no. B5, p. 7159–7182.

Harrison, T.M., Leloup, P.H., Ryerson, F.J., Tapponnier, P., Lacassin, R., and Chen, W., 1996, Diachronous initiation of transtension along the Ailao Shan–Red River shear zone, Yunnan and Vietnam, *in* Yin, A., and Harrison, T.M., eds., The tectonic evolution of Asia: New York, Cambridge University Press, p. 208–226.

Holt, W.E., Ni, J.F., Wallace, T.C., and Haines, A.J., 1991, The active tectonics of the Eastern Himalayan Syntaxis and surrounding regions: Journal of Geophysical Research, v. 96, no. B9, p. 14,595–14,632.

Howard, A.D., 1980, Thresholds in river regimes, *in* Coats, D.R., and Vitek, J.D., eds., Thresholds in geomorphology: Boston, Massachusetts, Allen and Unwin, p. 227–258.

Howard, A.D., 1994, A detachment-limited model of drainage basin evolution: Water Resources Research, v. 30, p. 2261–2285.

Howard, A.D., 1998, Long profile development of bedrock channels: Interaction of weathering, mass wasting, bed erosion, and sediment transport, *in* Tinkler, K., and Wohl, E.E., eds., Rivers over rock: Fluvial processes in bedrock channels: American Geophysical Union Geophysical Monograph 107, p. 297–319.

Kirby, E., and Whipple, K.X, 2001, Quantifying differential rock-uplift rates via stream profile analysis: Geology, v. 29, p. 415–418.

Kirby, E., Reiners, P.W., Krol, M.A., Whipple, K.X, Hodges, K.V., Farley, K.A., Tang, W., and Chen, Z., 2002, Late Cenozoic evolution of the eastern margin of the Tibetan Plateau: Inferences from $^{40}Ar/^{39}Ar$ and (U/Th)/He thermochronology: Tectonics, v. 21, no. 1, doi:10.1029/2000TC001246.

Kirby, E., Whipple, K.X, Tang, W., and Chen, Z., 2003, Distribution of active rock uplift along the eastern margin of the Tibetan Plateau: Inferences from bedrock channel longitudinal profiles: Journal of Geophysical Research, v. 108, doi:10.1029/2001JB000861.

Lague, D., and Davy, P., 2003, Constraints on the long-term colluvial erosion law by analyzing slope-area relationships at various tectonic uplift rates in the Siwalik Hills (Nepal): Journal of Geophysical Research, v. 106, no. B2, p. 26,561–26,591.

Leloup, P.H., and Kienast, J.R., 1993, High-temperature metamorphism in a major Tertiary ductile continental strike-slip shear zone: The Ailao Shan–Red River (P.R.C.): Earth and Planetary Science Letters, v. 118, p. 213–234.

Leloup, P.H., Lacassin, R., Tapponnier, P., Schärer, U., Zhong, D., Liu, X., Zhang, L., Ji, S., and Phan, T.T., 1995, The Ailao Shan–Red River shear zone (Yunnan, China), Tertiary transform boundary of Indochina: Tectonophysics, v. 251, p. 3–84.

Leloup, P.H., Arnaud, N., Lacassin, R., Kienast, J.R., Harrison, T.M., Phan Trong, T.T., Replumaz, A., and Tapponnier, P., 2001, New constraints on the structure, thermochronology, and timing of the Ailao Shan–Red River shear zone, SE Asia: Journal of Geophysical Research B, v. 106, p. 6683–6732.

Merrits, D.J., and Vincent, K.R., 1989, Geomorphic response of coastal stream to low, intermediate, and high rates of uplift, Mendocino junction region, northern California: Geological Society of America Bulletin, v. 101, p. 1373–1388.

Molnar, P., 2001, Climate change, flooding in arid environments, and erosion rates: Geology, v. 29, p. 1071–1074.

Phillips, J.D., 2002, Erosion, isostatic response, and the missing peneplains: Geomorphology, v. 45, p. 225–241.

Replumaz, A., Lacassin, R., Tapponnier, P., and Leloup, P.H., 2001, Large river offsets and Plio-Quaternary dextral strike-slip rate on the Red River fault (Yunnan, China): Journal of Geophysical Research B, v. 106, p. 819–836.

Royden, L.H., 1996, Coupling and decoupling of crust and mantle in convergent orogens: Implications for strain partitioning in the crust: Journal of Geophysical Research, v. 101, no. B8, p. 17,679–17,705.

Royden, L.H., Burchfiel, B.C., King, R.W., Wang, E., Chen, Z., Shen, F., and Liu, Y., 1997, Surface deformation and lower crustal flow in eastern Tibet: Science, v. 276, p. 788–790.

Royden, L.H., Clark, M.K., and Whipple, K.X, 2000, Evolution of river elevation profiles by bedrock incision: Analytical solutions for transient river profiles related to changing uplift and precipitation rates: Eos (Transactions, American Geophysical Union), v. 81, Fall Meeting Supplement, Abstract T62F-09.

Ruddiman, W.F., and Kutzbach, J.E., 1989, Forcing of Late Cenozoic northern hemisphere climate by plateau uplift in southern Asia and the American west: Journal of Geophysical Research, v. 94, p. 18,409–18,427.

Schärer, U., Zhang, L., and Tapponnier, P., 1994, Duration of strike-slip movements in large shear zones: the Red River belt, China: Earth and Planetary Science Letters, v. 126, p. 379–397.

Seidl, M.A., and Dietrich, W.E., 1992, The problem of channel erosion into bedrock, *in* Schmidt, K.H., and de Ploey, J., eds., Functional geomorphology: Catena, supplement 23, p. 101–124.

Seidl, M.A., Dietrich, W.E., and Kirchner, J.W., 1994, Longitudinal profile development into bedrock: An analysis of Hawaiian channels: Journal of Geology, v. 102, p. 457–474.

Sklar, L.S., and Dietrich, W.E., 1998, River longitudinal profiles and bedrock incision models: Stream power and the influence of sediment supply, *in* Tinkler, K., and Wohl, E.E., eds., Rivers over rock: Fluvial processes in bedrock channels: American Geophysical Union Geophysical Monograph 107, p. 237–260.

Sklar, L.S., and Dietrich, W.E., 2001, Sediment and rock strength controls on river incision into bedrock: Geology, v. 29, p. 1087–1090.

Snyder, N.P., Whipple, K.X, Tucker, G.E., and Merritts, D.J., 2000, Landscape response to tectonic forcing: DEM analysis of stream profiles in the Mendocino triple junction region, northern California: Geological Society of America Bulletin, v. 112, p. 1250–1263.

Spotila, J.A., and Sieh, K., 2000, Architecture of transpressional thrust faulting in the San Bernardino Mountains, southern California, from deformation of a deeply weathered surface: Tectonics, v. 19, p. 589–615.

Tapponnier, P., Peltzer, G., Armijo, R., Le Dain, A.-Y., and Cobbold, P., 1982, Propagating extrusion tectonics in Asia: New insights from simple experiments with plasticine: Geology, v. 10, p. 611–616.

Tapponnier, P., Peltzer, G., and Armijo, R., 1986, On the mechanics of the collision between India and Asia, *in* Coward, M.P., and Ries, A.C., eds., Collision tectonics: Geological Society [London] Special Publication 19, p. 115–157.

Tapponnier, P., Lacassin, R., Leloup, P.H., Schärer, U., Zhong, D., Liu, X., Ji, S., Zhang, L., and Zhong, J.,

1990, The Ailao Shan/Red River metamorphic belt: Tertiary left-lateral shear between Indochina and south China: Nature, v. 343, p. 431–437.

Tucker, G.E., and Whipple, K.X, 2002, Topographic outcomes predicted by stream erosion models: Sensitivity analysis and intermodel comparison: Journal of Geophysical Research, v. 107, doi:10.1029/2001JB000162.

U.S. Geological Survey, 1993, Digital elevation models, data user guide, 5: Reston, Virginia, U.S. Geological Survey, p. 1–50.

Wang, Erchie, and Burchfiel, B.C., 1997, Interpretation of Cenozoic tectonics in the right-lateral accommodation zone between the Ailao Shan shear zone and the Eastern Himalayan Syntaxis: International Geology Review, v. 39, p. 191–219.

Wang, Erchie, Burchfiel, B.C., Royden, L.H., Chen, L., Chen, J., Li, W., and Chen, Z., 1998, Late Cenozoic Xianshuihe-Xiaojiang, Red River and Dali fault systems of southwestern Sichuan and central Yunnan, China: Boulder, Colorado, Geological Society of America Special Paper 327, 108 p.

Wang, P.-L., Lo C.-H., Lee, T.-Y., Chung, S.-L., Lan, C.-Y., and Nguyen, T.-Y., 1998, Thermochronological evidence for the movement of the Ailao Shan–Red River shear zone: A perspective from Vietnam: Geology, v. 26, p. 887–890.

Wang, P.-L., Lo C.-H., Chung, S.-L., Lee, T.-Y., Lan, C.-Y., and Trang. V.-T., 2000, Onset timing of left-lateral movement along the Ailao Shan–Red River shear zone: $^{40}Ar/^{39}Ar$ dating constraint from the Nam Dinh Area, northeastern Vietnam: Journal of Asian Earth Sciences, v. 18, p. 281–292.

Weissel, J.K., and Seidl, M.A., 1998, Inland propagation of erosional escarpments and river profile evolution across the southeast Australian passive continental margin, *in* Tinkler, K., and Wohl, E.E., eds., Rivers over rock: Fluvial processes in bedrock channels: American Geophysical Union Geophysical Monograph 107, p. 189–206.

Whipple, K.X, 2001, Fluvial landscape response time; how plausible is steady-state denudation?: American Journal of Science, v. 301, p. 313–325.

Whipple, K.X, 2004, Bedrock rivers and the geomorphology of active orogens: Annual Review of Earth and Planetary Sciences, v. 32, 10.1146/annurev.earth.32.101802.120356.

Whipple, K.X, and Tucker, G.E., 1999, Dynamics of the stream-power river incision model: Implications for height limits of mountain ranges, landscape response timescales, and research needs: Journal of Geophysical Research, v. 104, no. B8, p. 17,661–17,674.

Whipple, K.X, and Tucker, G.E., 2002, Implications of sediment-flux-dependent river incision models for landscape evolution: Journal of Geophysical Research, v. 107, no. B2, doi:10.1029/2000JB000044.

Widdowson, M., 1997, The geomorphological and geological importance of paleosurfaces, *in* Widdowson, M., ed., Paleosurfaces: Recognition, reconstruction and paleoenvironmental interpretation: Geological Society [London] Special Publication 120, p. 1–12.

Wobus, C.W., Hodges, K.V., and Whipple, K.X, 2003, Has focused denudation sustained active thrusting at the Himalayan topographic front?: Geology, v. 31, p. 861–864.

Xu, G., and Kamp, P.J.J., 2000, Tectonics and denudation adjacent to the Xianshuihe fault, eastern Tibetan plateau: Constraints from fission track thermochronology: Journal of Geophysical Research B, v. 105, p. 19,231–19,251.

Zhang, L.-S., and Schärer, U., 1999, Age and origin of magmatism along the Cenozoic Red River shear belt, China: Contributions to Mineralogy and Petrology, v. 134, p. 67–85.

Manuscript Received by the Society 25 March 2003
Revised Manuscript Received 16 November 2003
Manuscript Accepted 29 November 2003

Printed in the USA